Geophysical Research Letters

RESEARCH LETTER
10.1029/2021GL093410

Revealing High-Manganese Material on Mars at Microscale

Xiaojia Zeng[1,2], Yanxue Wu[3], Yuyan S. Zhao[1,2,4], Runlian Pang[5], Bing Mo[1,2,4], Yuanyun Wen[1,2,4], Xiongyao Li[1,2,4], and Jianzhong Liu[1,2,4]

[1]Center for Lunar and Planetary Sciences, Institute of Geochemistry, Chinese Academy of Sciences, Guiyang, China, [2]Key Laboratory of Space Manufacturing Technology, Chinese Academy of Sciences, Beijing, China, [3]Analysis and Test Center, Guangdong University of Technology, Guangzhou, China, [4]CAS Center for Excellence in Comparative Planetology, Hefei, China, [5]State Key Laboratory of Ore Deposit Geochemistry, Institute of Geochemistry, Chinese Academy of Sciences, Guiyang, China

Abstract High-manganese materials would provide valuable information about the history of a water-rich and oxidizing environment on early Mars. However, the detailed texture and components of these high-manganese materials are unknown. In martian breccia meteorite NWA 11220, one unique lithic clast enriched in high-manganese material (~5 vol%) has been recognized. Here, we report the morphological, micro-textural, mineralogical, and geochemical features of the martian high-manganese material at the microscale for the first time. Our results show that (a) high-manganese materials are characterized by micron-sized grain (<50 μm), complex associated-phase (i.e., apatite, enstatite, magnetite, ilmenite, and amorphous matrix), and chemical heterogeneity; (b) nano-sized (<500 nm) amorphous manganese-oxide veins or grains are the only manganese-bearing phases in the high-manganese materials. These new observations provide new evidence for revealing the geological processes related to the high-manganese materials on Mars and provide important information for future *in-situ* exploration and data interpretation of high-manganese materials on Mars.

Plain Language Summary On Earth, the presence of high-manganese concentrations is commonly thought to be an indicator of water-rich and highly oxidizing conditions. Similarly, high-manganese materials have also been detected on Mars at the Curiosity/Opportunity landing sites and within a martian breccia meteorite. Knowledge of the components of these high-manganese materials would provide important information about the environments in which they formed on Mars. However, the detailed texture and components of these high-manganese materials from Mars are still unclear. Based on a unique lithic clast enriched in high-manganese material (~5 vol%) from martian breccia meteorite NWA 11220, the morphology, texture, mineralogy, and geochemistry of the martian high-manganese material were revealed at the microscale for the first time. These supplementary data provide a series of new insights into the high-manganese material on Mars, including (a) the new occurrence of manganese concentration in martian igneous rocks, (b) micro-textural evidence of fluid precipitation of high-manganese material, and (3) geological history recorded by high-manganese materials on Mars.

Xiaojia Zeng and Yanxue Wu contributed equally to this work.

Key Points:

- One unique lithic clast enriched in high-Mn material (~5 vol%) was identified in martian breccia meteorite NWA 11220
- The texture, geochemistry, and mineralogy of the high-Mn material on Mars are reported at the microscale
- Nano-sized (<500 nm) amorphous Mn-bearing material veins or grains are the only Mn-bearing phase in the high-Mn material

Supporting Information:

Supporting Information may be found in the online version of this article.

Correspondence to:

X. Li and J. Liu,
lixiongyao@vip.skleg.cn;
liujianzhong@mail.gyig.ac.cn

Citation:

Zeng, X., Wu, Y., Zhao, Y. S., Pang, R., Mo, B., Wen, Y., et al. (2021). Revealing high-manganese material on Mars at microscale. *Geophysical Research Letters*, *48*, e2021GL093410. https://doi.org/10.1029/2021GL093410

Received 17 MAR 2021
Accepted 12 AUG 2021

1. Introduction

Manganese (Mn) is a redox-sensitive element. It commonly occurs as Mn(II) (substituting for Fe^{2+}) in a wide range of primary igneous minerals (e.g., olivine and pyroxene). On Earth, when igneous rocks interact with surface water or groundwater, Mn is readily depleted from the host rock and becomes mobile, as Mn(II), in aqueous systems (Crerar et al., 1980). To precipitate and concentrate Mn, the reduced Mn^{2+} needs to be oxidized by high-potential oxidants (much higher than that for Fe or S, e.g., O_2) in liquid water to form insoluble high-valence Mn-oxides (e.g., Lanza et al., 2014; Post, 1999; Tebo et al., 2005). Thus, the presence of high Mn concentrations is commonly thought to be an indicator of water-rich and highly oxidizing conditions (e.g., Lanza et al., 2016; Maynard, 2010; Post, 1999).

On Mars, high-Mn materials have been recently discovered by the Curiosity and Opportunity rovers in Gale Crater and Endeavour Crater, respectively (e.g., Arvidson et al., 2016; Lamm et al., 2018; Lanza et al., 2014, 2016). In Gale Crater, the high-Mn materials were observed in a variety of geologic settings,

including as a surface coating, fracture fill, and embedded in fine-grained sediments (Lanza et al., 2014; 2016; Meslin et al., 2018). Opportunity has detected a rock fragment (i.e., Pinnacle Island) with an average MnO content of 2.38 wt% (Arvidson et al., 2016). In addition, high-Mn materials have also been discovered in martian breccia regolith meteorites from Northwest Africa (NWA) 7034/7533 (Liu et al., 2017, 2021). They occur as nanocrystalline aggregates in diverse petrographic contexts (e.g., perthite-rich clast, spherules, and matrix). Synchrotron analyses have revealed that the majority of the Mn in high-Mn materials is IV+, with varying smaller amounts of III+ (Liu et al., 2017, 2021).

A mineralogical context for the high-Mn material on Mars would provide essential clues pointing toward the oxidation states of the Mn-phases, aqueous environments, and atmospheric condition on early Mars (Lanza et al., 2016; Noda et al., 2018). However, until now, the micro-textures and components of the high-Mn materials on Mars have remained unclear. *In-situ* measurements conducted by Curiosity have shown that the high-Mn materials on Mars occur either within thin fractures (Lamm et al., 2018) or as fine-grained sediments (typical grain size <100 μm) (Lanza et al., 2016). This leads to great challenges in analyzing their mineralogical information using the mineralogical tools onboard the Curiosity and Opportunity rovers (e.g., Alpha Particle X-ray Spectrometer (APXS) and Chemistry and Camera complex (ChemCam), which have analysis spot sizes of >350–500 μm and >1.7 mm, respectively; Lanza et al., 2014). The synchrotron analyses of the high-Mn material in martian breccia meteorite NWA 7034/7533 suggest that the material is nanocrystalline aggregate, making it difficult to identify the Mn-bearing phases using such techniques (Liu et al., 2017, 2021).

Recently, one lithic clast enriched in high-Mn material was identified in martian breccia meteorite NWA 11220 (paired with NWA 7034; Figure S1). This lithic clast has an igneous monzonite lithology, and it is distinctly characterized by containing ~5 vol% of high-Mn material (Figure 1). Such a unique rock fragment provides an opportunity to analyze the high-Mn material in the laboratory using high-resolution micro-probe techniques (e.g., a transmission electron microscope). In this study, we describe the occurrence and petrology of the unique martian lithology enriched in high-Mn material, and then, we investigate the textural, mineralogical, and geochemical features of the high-Mn material at the microscale. Furthermore, the formation and geological history of the high-Mn material on Mars is constrained using the new microscale data.

2. Sample and Analytical Methods

NWA 11220 is a martian regolith breccia meteorite, which is paired with NWA 7034 and its pairs (Stephen, 2018). Previous studies have described the petrology, mineralogy, geochemistry, and chronology of this group of meteorites (e.g., Agee et al., 2013; Hewins et al., 2017; Wittmann et al., 2015). The polished thick section of NWA 11220 was prepared at the Institute of Geochemistry, Chinese Academy of Sciences (Figure S1). In this meteorite, one unique lithic clast (called "Clast-MN1"; Figures 1 and S1) enriched in high-Mn material was identified. Then, the high-Mn material in this clast was characterized using a wide range of *in-situ* analytical techniques.

Back-Scattered Electron (BSE) images were collected using the FEI Scios Dual-Beam Focused Ion Beam/Scanning Electron Microscope (FIB/SEM) at the Institute of Geochemistry, Chinese Academy of Sciences. The operating conditions were a 15–20 kV accelerating voltage and a 0.8–1.6 nA beam current. Semi-quantitative compositional analyses and X-ray elemental mapping of this clast were also performed using the same FEI Scios FIB/SEM and an energy dispersive detection system (EDS of EDAX), with the same voltage and current setting noted above. To estimate the mineral abundance of Clast-MN1, the BSE images and X-ray elemental maps were analyzed using Adobe Photoshop to count the pixels of the different phases. Then, the modal mineralogy (vol%) of Clast-MN1 was calculated. Mineral chemistry of Clast-MN1 was analyzed using Electron MicroProbe Analysis (EMPA) (JXA 8230) at the Guilin University of Technology (Table S1 and Figure S2). The operating conditions were a 15 kV accelerating voltage and a 20 nA beam current, with a 2–5 μm defocused beam. Natural and synthetic standards were used, and matrix corrections were made based on ZAF procedures. The typical detection limits were ~0.01–0.03 wt%.

Two ultra-thin foils of high-Mn material (Figures S3 and S4) in Clast-MN1 were prepared using the FIB/SEM (FEI Scios) at the Institute of Geochemistry, Chinese Academy of Sciences, following the methods of

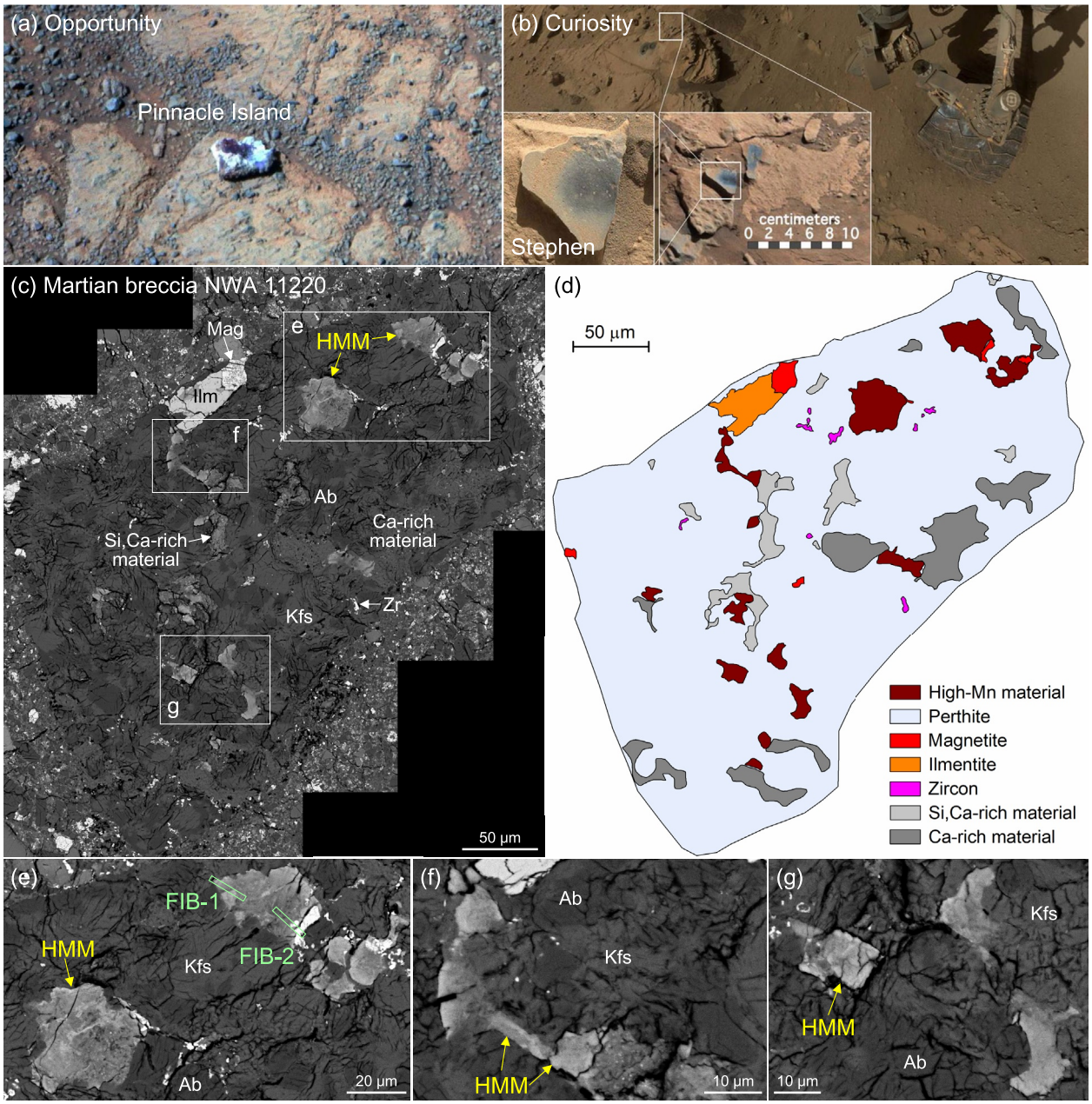

Figure 1. High-Mn materials on Mars. (a) Pinnacle Island with 2.38 wt% MnO detected by Opportunity (Arvidson et al., 2016). The Pancam image was acquired on sol 3540 by Opportunity rover (Pancam product ID: 1P442453229RADCAEFP2594l5C1). (b) High-Mn target Stephen observed by Curiosity (Lanza et al., 2016). This image includes Mars Hand Lens Imager (MHLI) self-portrait of Curiosity in front of the Windjana site (NASA image PIA 18390), Mastcam-Right image of Stephen (0626ML0026760010302385E01), and MAHLI image of Stephen (0627MH0001900010203555C00). (c) Back-Scattered Electron image of the studied unique martian lithology (i.e., Clast-MN1) enriched in high-Mn material from martian breccia meteorite NWA 11220. (d) Cartoon showing the mineralogy of Clast-MN1. (e–g) Close-ups of the regions marked in panel (c). The distinctive feature of Clast-MN1 in NWA 11002 is that this clast contains ~5 vol% high-Mn material, with grain sizes ranging from ~2 to 50 μm. Mineral phases in Clast-MN1 are labeled: HMM = high-Mn material, Kfs = K-feldspar, Ab = albite, Ilm = ilmenite, Mag = magnetite, and Zr = zircon.

Zeng et al. (2020). The micro-textural, mineralogical, and geochemical features of the prepared FIB foils of the high-Mn material were analyzed (Figures S5–S7) using the Field-Emission Transmission Electron Microscope (FE-TEM; FEI Talos F200S) equipped with an EDX system (xflash 6T 30) at the Guangdong University of Technology. The analyses were conducted at a 200 kV accelerating voltage and a 1–2 nA beam current. Bright-field TEM observations, energy-dispersive X-ray analyses, and high-angle annular dark

field-scanning transmission electron microscope (HAADF-STEM) observations were performed using this instrument.

In addition, Raman spectra of the P, Ca, and Cl-rich grains recognized in the high-Mn material was measured using Renishaw (RM 2000 and inVia Plus) micro-Raman spectrometers with a CCD detector at the Institute of Geochemistry, Chinese Academy of Sciences. The 50X objective was used to focus the excitation beam to a <1- μm spot. The laser (532 nm) energy was 50 mW. Raman spectra were acquired with the following conditions: 1% power of the laser energy, 200−1,200 cm^{-1} spectra range, and 20 s exposure time. Silicon (520.7 cm^{-1} Raman shift) was used as a standard to calibrate the instrument during the measurements.

3. Results

3.1. Occurrence of High-Mn Material in Clast-MN1

In martian breccia NWA 11220, one lithic clast enriched in high-Mn material (i.e., Clast-MN1) was identified in the matrix of this meteorite (Figures 1 and S1). This clast is 400 × 300 μm in size and exhibits an igneous texture. Mineralogically, Clast-MN1 is perthite-rich and is mainly composed of ~37 vol% K-feldspar ($An_{1.4–3.1}Ab_{6.8–18.3}Or_{78.6–91.6}$), ~45 vol% albite ($An_{2.1–7.0}Ab_{88.9–81.9}Or_{4.5–14.2}$), ~2 vol% opaque phases (e.g., ilmenite and magnetite), and ~5 vol% high-Mn materials. In addition, ~10 vol% Si, Ca-rich, and Ca-rich materials were also observed in Clast-MN1 (Figures 1 and S2; Table S1). The high-Mn materials in Clast-MN1 commonly occur as irregular grains or as elongated laths, with grain sizes ranging from ~2 to 50 μm (Figure 1c). Most of the high-Mn materials contain fracture, which commonly cut across the surrounding K-feldspar/albite (Figures 1e–1g).

3.2. Micro-Texture of High-Mn Material

Micro-texture and morphology of the high-Mn material were investigated using the BSE images and HAADF-STEM images (Figures 1, 2, S3, and S4). The results show that the high-Mn materials in Clast-MN1 have relatively sharp boundaries with the surrounding mineral phases (e.g., plagioclase) (Figures 2, S3, and S4). No replacement texture was observed at micro-scale in the high-Mn material (Figure 2). Plagioclase grains associated with the high-Mn material commonly contain fracture-networks (<1 μm in width), while only a few fractures were observed in the high-Mn material (Figures 1e–1g). Mn-rich phase in the high-Mn materials occurs as either Mn-rich vein-like phases or Mn-rich nano-crystalline aggregates (<100 nm). Some of the vein-like Mn-rich phases fill the fractures in the K-feldspar (Figures 2, S3, and S4). In addition, numerous submicron-sized (<500 nm) pores were observed in the studied FIB foils of the high-Mn material (Figure 2).

3.3. Amorphous Mn-Bearing Material Identified in High-Mn Material

TEM observations revealed that the Mn-rich phase that occurs in the high-Mn material is amorphous. No Mn-rich crystals (e.g., bixbyite Mn_2O_3 and pyrolusite MnO_2) were detected in the FIB slices of the high-Mn material (Figures 2 and 3). These amorphous Mn-bearing materials occur as nanometer-sized (<10 nm) veins or amorphous grains (<500 nm in width) (Figure 2). Texturally, these amorphous Mn-bearing material veins cut across the high-Mn materials or fill the fractures in the surrounding K-feldspar (Figures 2, S3, and S4). However, the Mn-rich nanometer-sized grains are unevenly distributed in the high-Mn materials (Figures 2, S3, and S4). The TEM-EDS results revealed that the amorphous Mn-bearing materials are mainly composed of ~5.66 wt% Mg, ~1.60 wt% Al, ~1.74 wt% Si, ~2.07 wt% Ca, ~45.8 wt% Mn, and ~41.1 wt% O (Table 1).

3.4. Minerals Recognized Within High-Mn Material

On the SEM-EDS X-ray element composition maps, one ~5 μm grain in the high-Mn material was observed to be enriched in Ca, P, and Cl (Figure 4). This grain was identified as apatite using the micro-Raman technique (Figures 4 and S8). In addition, the TEM-EDS X-ray element mapping results revealed the presence of a vein-like C, Ca-rich phase, and a Mg, Fe, Si-rich phase in the high-Mn materials (Figures 2, S5, and S6).

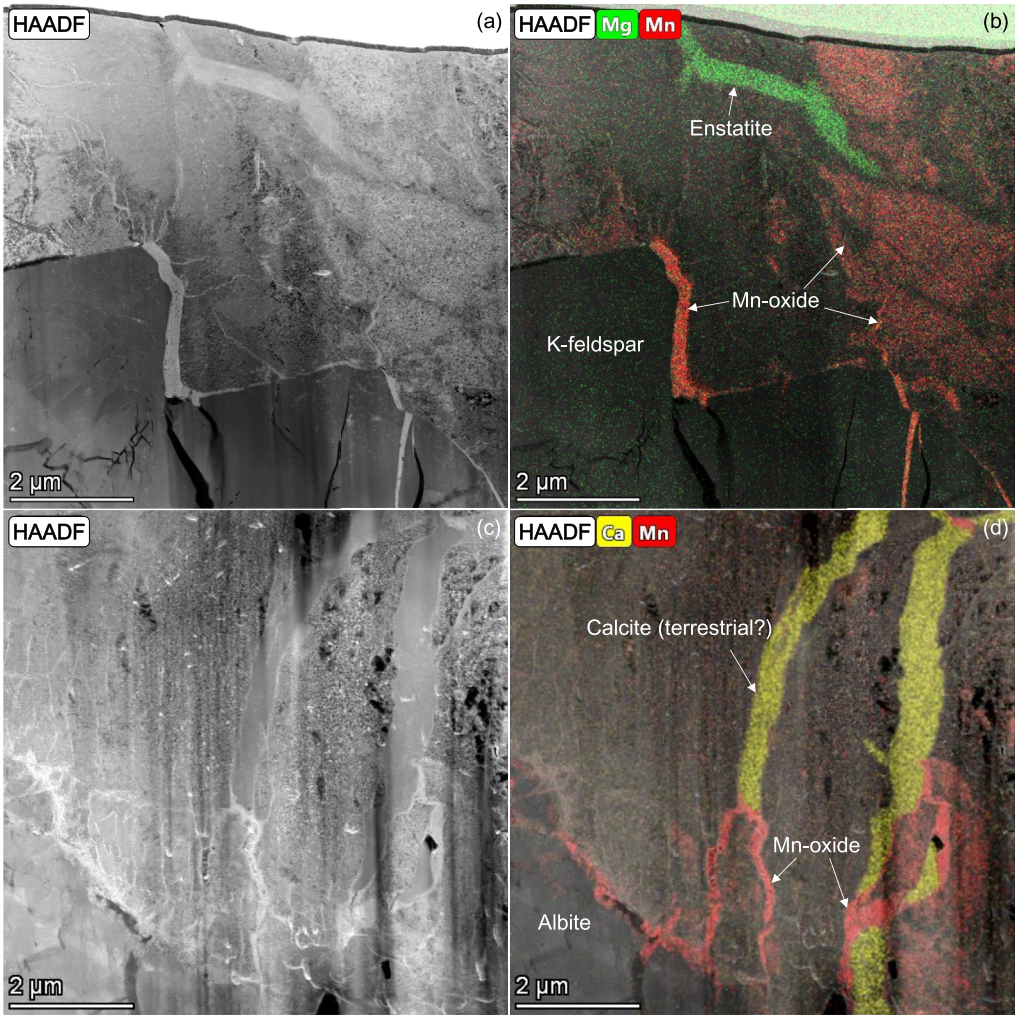

Figure 2. Micro-texture of the high-Mn material in Clast-MN1. (a and b) Representative HAADF image and TEM-EDS X-ray mapping results for slice FIB-1. (c and d) Representative HAADF image and TEM-EDS X-ray mapping results for slice FIB-2. Mn-oxides in the high-Mn material occur as either nano-sized (<10 nm) grains or veins (<500 nm in width). Some veins of Mn-oxide fill into the fractures of the associated feldspar crystal. No replacement texture between the Mn-oxide and the surrounding feldspar is observed.

Based on the TEM-EDS and TEM SAED data, these phases were identified as calcite and enstatite, respectively (Figure S7). In addition, the ilmenite and magnetite grains were also observed to be associated with the high-Mn material in Clast-MN1 (Figures 1 and 4).

3.5. Chemical Heterogeneity of High-Mn Material

As can be seen from the BSE images, the high-Mn material in Clast-MN1 exhibit varying brightness (i.e., dark area and bright area; Figure 4), suggesting that they are chemically heterogeneous at micron-scale. This conclusion is supported by the X-ray element mapping results for the ~50 μm high-Mn material (Figure 4). Specifically, some areas of this grain are rich in Fe, Al, and Mn, while other areas are rich in Mg, Si, and Ca (Figure 4). The EDS analyses of the high-Mn materials revealed that they contain ~0.78–1.30 wt% Mg, ~2.24–7.27 wt% Al, ~8.88–21.5 wt% Si, ~0.00–0.71 wt% P, ~0.00–0.47 wt% Cl, ~0.12–7.16 wt% K, ~3.67–7.61 wt% Ca, ~1.53–21.3 wt% Mn, and ~6.71–28.0 wt% Fe (Table 1).

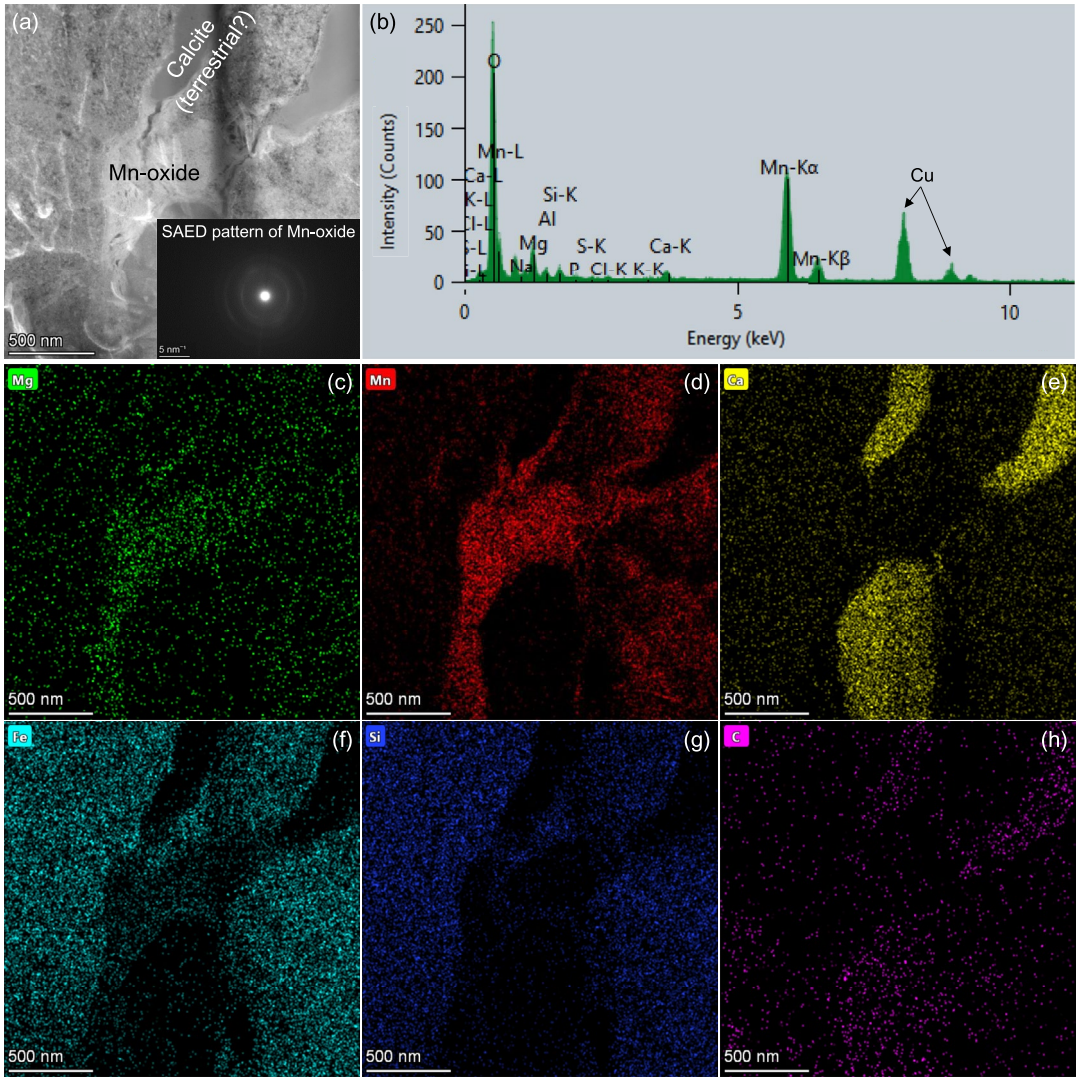

Figure 3. The amorphous Mn-bearing material identified in high-Mn material from Clast-MN1. (a) HAADF image of the amorphous Mn-bearing material. SAED pattern of this amorphous material is also shown in this image. (b) Representative TEM-EDS result for the amorphous Mn-bearing material. The peaks of Cu in the EDS spectrum are of artificial origin during the preparation of FIB foils that were mounted onto a TEM copper grid. (c–h) TEM X-ray mapping results (i.e., Mg, Mn, Ca, Fe, Si, and C) for the amorphous Mn-bearing material. The amorphous Mn-bearing material are the only Mn-bearing phase in high-Mn material. No Mn-bearing crystals are observed in the high-Mn material.

4. Discussion and Implications

Martian breccia NWA 11220 is a hot desert meteorite, which would have been altered by terrestrial weathering processes on Earth (Saunier et al., 2010; Gattacceca et al., 2019). However, the texture and mineralogy of the high-Mn materials in Clast-MN1 indicate that they would be of Mars origin, rather than terrestrial weathering products in hot desert. The evidence for this conclusion includes the following: (a) Manganese is a trace element in martian silicate minerals (e.g., olivine and plagioclase), and the Mn contents of the martian Fe-Ti oxides are only up to ~3 wt% (e.g., Santos et al., 2015). Such low Mn contents in martian minerals cannot explain the high Mn abundance in the studied Mn-oxides (i.e., Mn = 45 wt%; Table 1). In addition, no weathering textures (e.g., decomposition) of silicate and Fe-Ti oxides were observed in breccia meteorite NWA 11220; (b) Many fractures were observed to cut through the high-Mn materials in Clast-MN1, and some of them also extend into their host minerals (i.e., K-feldspar and albite; Figures 1e–1g). This texture indicates that the high-Mn materials were formed before NWA 11220 was ejected from Mars

Table 1
Representative Chemical Results of High-Mn Material (SEM-EDS) and Mn-Oxide (TEM-EDS) in Clast-MN1 From Martian Breccia NWA 11220

	High-Mn material (wt%)							Amorphous Mn-bearing material		
	1	2	3	4	5	Range	Average		at%	wt%
O	47.4	49.8	47.3	40.3	46.6	40.3–49.8	46.3	O	66.2	41.1
Mg	0.78	1.07	1.30	0.87	0.95	0.78–1.30	0.99	Na	0.97	0.86
Al	7.27	3.58	2.47	2.24	2.72	2.24–7.27	3.66	Mg	6.00	5.66
Si	21.5	12.6	12.6	9.20	8.88	8.88–21.5	13.0	Al	1.53	1.60
P	n.d.	0.36	0.71	n.d.	n.d.	n.d.—0.71	0.53	Si	1.60	1.74
Cl	n.d.	0.36	0.47	0.12	0.24	n.d.—0.47	0.30	P	0.22	0.26
K	7.16	0.48	0.47	0.12	0.36	0.12–7.16	1.72	S	0.15	0.19
Ca	7.61	3.93	5.06	4.48	3.67	3.67–7.61	4.95	Cl	0.35	0.48
Mn	1.57	5.96	1.53	21.3	17.9	1.53–21.3	9.64	K	0.14	0.21
Fe	6.71	21.8	28.0	21.4	18.7	6.71–28.0	19.3	Ca	1.33	2.07
								Mn	21.5	45.8

Note. High-Mn materials show relatively large compositional variation, because they are composed of complex submicron (<1 μm) phases (e.g., enstatite, amorphous material, and calcite). Manganese abundance in the amorphous Mn-bearing material reaches up to 45.8 wt%.
n.d. = not detected.

and/or fell to the Earth because terrestrial weathering products commonly fill the pre-existing fractures in meteorites; (c) Previous works showed that the alteration of hot desert meteorites is mineralogically characterized by the replacement of primary Fe^0- and Fe^{2+}- minerals (e.g., Fe-Ni metal, troilite, and silicates) by weathering products (e.g., goethite, lepidocrocite, barite, and gypsum; Bland et al., 2006; Hyde et al., 2014; Lee & Bland, 2004). No Mn-rich mineral phases (e.g., Mn > 20 wt%) were recognized as terrestrial products within desert meteorites, because of the relatively low Mn content in the primary Fe^0- and Fe^{2+}- minerals (e.g., Fe-Ni metal, troilite, and silicates). For the mineral assemblage of high-Mn material (e.g., apatite, enstatite, and amorphous Mn-bearing material; Figure 2) in Clast-MN1, these mineral phases are not the typical terrestrial weathering products of the desert meteorites (e.g., chondrites or lunar meteorites; Bland et al., 2006; Hyde et al., 2014; Lee & Bland, 2004). It is reasonable to indicate that the high-Mn material cannot be explained by the terrestrial processes on the Earth; and (d) In particular, Mn-rich glasses (Mn = 4.8–5.6 wt%) have been observed in the fusion crust of the breccia meteorite NWA 7034 (Liu et al., 2021). This provides a direct and critical evidence for the martian origin of high-Mn material in this meteorite. For the calcite observed in high-Mn material (Figure 2), it is hard to determine whether this mineral is from the Earth or Mars (because of the lack of geochemical evidence, e.g., the oxygen isotope data). Texturally, the calcite veins in high-Mn material are morphologically smooth and are free of fractures/pores (Figure 2). Such features are consistent with the terrestrial-contaminated calcite in desert meteorites (e.g., Al-Kathiri et al., 2005; Roszjar et al., 2011). However, calcite has also been observed in martian meteorites (e.g., ALH 84001; Thomas-Keprta et al., 2009) and on the surface of Mars (Ehlmann & Edwards, 2014). The martian origin of calcite in Clast-MN1 is also possible; more geochemical evidence, in future work, would be helpful to give clues about its origin.

In this study, new observations of high-Mn materials at microscale provided a series of new insights into this material on Mars. These mainly include the following: (a) Unlike the high-Mn material observed within sedimentary rocks by Curiosity rover (e.g., Lanza et al., 2014, 2016, 2019, 2021; Meslin et al., 2018), Clast-MN1 represents an igneous martian rock fragment containing high-Mn material on Mars. In martian breccia NWA 7034 and NWA7533, the Mn-rich regions were observed in four types of lithological contexts, including monzonite clasts, pyroxene clumps, basalts, and altered Fe-Ti oxides (Liu et al., 2021). Mineralogically, Clast-MN1 is consistent with the Mn-bearing monzonite clasts in NWA 7034 and NWA 7533. However, Clast-MN1 contains more abundance of high-Mn material (~5 vol%) than that in these previously

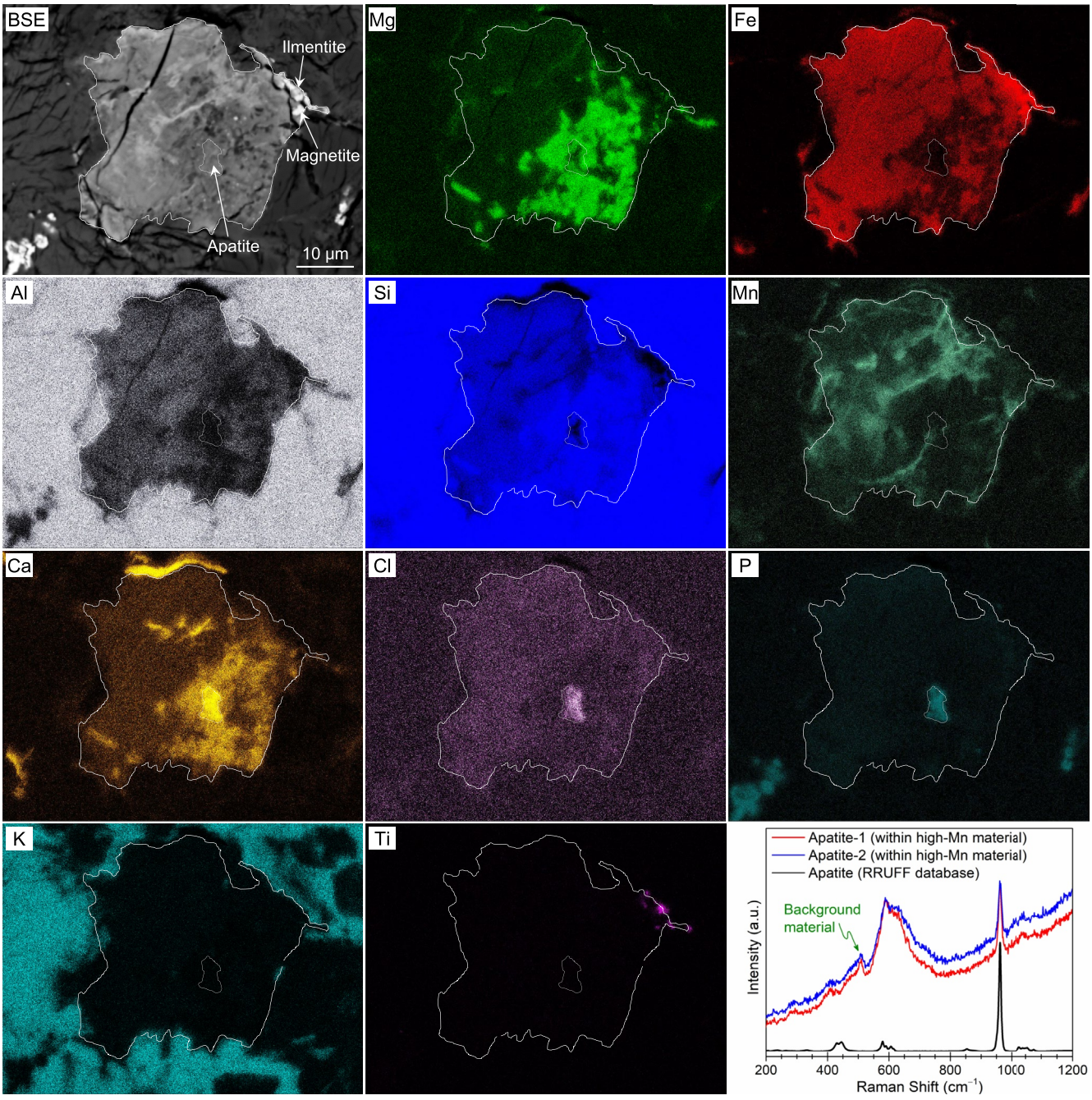

Figure 4. Back-Scattered Electron image and X-ray element composite maps of the ~50 μm high-Mn material observed in Clast-MN1. These elemental maps show that high-Mn material is chemically and mineralogically heterogeneous at the micron scale. The Ca, P, Cl,-rich grain within high-Mn material is identified as the apatite by the Raman spectra (see the image in the lower right corner). Ilmenite and magnetite grains are also observed associated with the high-Mn material.

reported Mn-bearing monzonite clasts (0.3–1 vol%; Liu et al., 2021); (b) Liu et al. (2017, 2021) suggested that the Mn-rich phase in high-Mn materials may be either birnessite or vernadite. Our TEM observations show that amorphous Mn-bearing material (poorly crystallized Mn-phase?) is the only Mn-bearing phase in the high-Mn materials on Mars. No Mn-bearing crystals were detected in the high-Mn material. The identification of various Mn-bearing phases in martian breccia suggests that the formation of high-Mn materials on Mars is a complex and diverse process; (c) This study reveals that martian high-Mn materials consist of complex minerals, including apatite, magnetite, ilmenite, and enstatite; (d) Considering the

micron size (i.e., <500 nm) of the Mn-rich phase, it is reasonable to suggest that the geochemical results of the high-Mn material conducted by Curiosity rover (Lanza et al., 2016) would be a mixed signal, which is most likely to be interfered by other materials; (e) ChemCam geochemical results of the high-Mn sediments show that there is no clear correlation between the Mn abundance and other elements (i.e., MgO and FeO) for the sample in Gale Crater (Lamm et al., 2018). Lamm et al. (2018) suggested that the Mn-bearing phase is likely an oxide phase rather than being associated with other major or minor elements. In this work, the identification of amorphous Mn-bearing material in high-Mn materials support this interpretation; (f) Recently, ChemCam results suggested that phosphorus was detected in 33% of Mn-rich nodular features at Groken drill site, Gale Crater (Lanza et al., 2021). Our observation of apatite within high-Mn material (Figures 4 and S8) would account for the increase in phosphorus observed in the Mn-rich nodule; and (g) Co-enrichments of Ni and Zn with Mn were observed by Curiosity and Opportunity rovers (Arvidson et al., 2016; Lanza et al., 2016). These observations and laboratory experiments (Noda et al., 2019) suggested that the high-Mn phases would be MnO_2. By comparison, the Ni and Zn contents in the studied Mn-bearing material is below the detection limit of TEM-EDS technique. This study found that the trace elements in Mn-bearing material include Na, P, S, Cl, and K (Table 1).

The texture of the amorphous Mn-bearing material provides information about its formation processes. Texturally, the amorphous Mn-bearing material mainly occurs as amorphous Mn-bearing material veins, which also fill the nearby K-feldspar fractures (Figure 2). This feature directly implies that fluid precipitation was the formation mechanism of the amorphous Mn-bearing material in Clast-MN1. Such conclusion is in agreement with the interpretation of the high Mn concentrations in the fracture networks observed by Curiosity rover on Mars (Lanza et al., 2016). On the Earth, Mn-oxide minerals commonly occur only as fine-grained, poorly crystalline aggregates and coatings (e.g., Post, 1999). This is consistent with the amorphous Mn-bearing material identified in Clast-MN1 (Figure 3), probably suggesting that the formation of Mn-oxide on Mars may be similar to that on the Earth.

Precipitation of high-Mn material generally requires highly oxidizing conditions and sufficient liquid water (Lanza et al., 2014; Post, 1999; Tebo et al., 2005). Previous studies have concluded that O_2 is the most likely oxidant for Mn oxidation and enrichment on Mars (Lanza et al., 2016; Liu et al., 2021). Our observations of the high-Mn material (e.g., amorphous Mn-bearing material vein, lack of oxychlorine, and fracture-filled texture) in Clast-MN1 are consistent with this suggestion. The atmospheric O_2 would be supplied to the groundwater through the hydrological cycle on ancient Mars. Then, this highly oxidizing groundwater would move along the pre-existing fractures in Clast-MN1, and transport the soluble Mn^{2+} cations (Mn^{2+} is substantially more soluble than Mn^{3+} and/or Mn^{4+}). The source of the Mn^{2+} could be the dissolution of the Mn^{2+}-bearing materials (e.g., silicate and ilmenite) that are widely distributed on Mars (Ehlmann & Edwards, 2014). Subsequently, high-Mn material (Mn^{3+} and/or Mn^{4+}) would be precipitated from the fluid under highly oxidizing conditions on Mars (Koyama et al., 2021; Wordsworth et al., 2021). Because the apatite grain has been recognized within the high-Mn material (Figure 4), it is reasonable to suggest that the fluids that deposited the Mn-oxides are not acidic (Hurowitz & McLennan, 2007).

Knowledge of the geological context of the high-Mn materials on Mars would provide information to constrain their geological history. Because high-Mn materials were observed in the lithic Clast-MN1 from breccia NWA 11220, it is reasonable to imply that the high-Mn material in NWA 11220 would be formed prior to the lithification of this breccia meteorite (i.e., ~1.5 Ga; McCubbin et al., 2016). Such late Amazonian age could be considered as the lower limit for the presence of high-Mn material on Mars. By contrast, the Noachian-aged Gale and Endeavour Craters would be considered as the upper limit for the formation of high-Mn materials on Mars (Crumpler et al., 2020; Wray, 2013). Accordingly, we suggest that the high-Mn material would be formed at Amazonian to Noachian period of Mars (i.e., ~1.5–3.8 Ga). In this work, the identification of the unique martian igneous Clast-MN1, which is enriched in high-Mn material (~5 vol%), from breccia NWA 11220 adds to the growing evidence for the presence of high-Mn material on Mars. Based on a comparison of the composition of NWA 7034 (paired with NWA 11220) with Mars global geochemical data, this meteorite is thought to be probably ejected from the Terra Sirenum region (30°S/165°W) in the southern highlands on Mars (Wittmann et al., 2015). This location is far from the landing sites of the Curiosity and Opportunity rovers (i.e., Gale and Endeavour Craters). This indicates that high-Mn material may be more widely distributed on Mars than previously thought.

For the *in-situ* detection of high-Mn materials on Mars, the previously available instruments (e.g., ChemCam and APXS) carried by Curiosity and Opportunity rovers are not applicable to the characterization of the micron-sized (<50 μm) high-Mn materials because of their relatively large analytical size (>350–500 μm footprint for ChemCam and >1.7 cm footprint for APXS). By comparison, the Scanning Habitable Environments with Raman and Luminescence for Organics and Chemicals (SHERLOC), a robotic arm-mounted instrument on NASA's Perseverance rover, is capable to detect minerals with the grain size of 50 μm (Bhartia et al., 2021). This instrument will be used to assess the geological history at Jezero crater through the identification of alteration minerals with Raman technique. Recently, Bernardini et al. (2021) demonstrated that Raman is a reliable method for determining the oxidation state of Manganese at the microscale. This suggests that the Perseverance rover is expected to obtain *in-situ* Raman data for high-Mn material on Mars. In the future, characterizing high-Mn materials from martian meteorites (or Mars return samples) in the laboratory with various instruments will improve our understanding of the high-Mn materials on Mars. For example, measurements of trace elements for high-Mn material using Nanoscale Secondary Ion Mass Spectrometry (Nano-SIMS) and the detection of water (OH) signal for high-Mn material with Micro-FTIR (Fourier Transform Infrared) spectroscopy.

Data Availability Statement

The image data of Opportunity and Curiosity rovers in this paper are archived at the NASA Planetary Data System (https://pds-imaging.jpl.nasa.gov; The links are https://pds-geosciences.wustl.edu/mer/mer1-m-pancam-3-radcal-rdr-v1/mer1pc_1xxx/data/sol3540/; https://pdsimage2.wr.usgs.gov/archive/MSL/MSLMST_0007/DATA/RDR/SURFACE/0626/; https://pdsimage2.wr.usgs.gov/archive/MSL/MSLMHL_0007/DATA/RDR/SURFACE/0627/). The measured petrological, mineralogical, and geochemical data used in this work is available in Zeng et al. (2021).

Acknowledgments
This research was supported by the B-type Strategic Priority Program of the Chinese Academy of Sciences (No. XDB41000000), National Natural Science Foundation of China (Nos. 41941003, 41931077, and 42103036), Pre-research project on Civil Aerospace Technologies by CNSA (No. D020201), Youth Innovation Promotion Association CAS (2014359), Key Research Program of Frontier Sciences CAS (No. QYZDY-SSW-DQC028), and China Postdoctoral Science Foundation to X. Zeng. We are grateful to Andrew J. Dombard for the editorial handling of the manuscript, and we thank Nina Lanza and the other two anonymous reviewers for their helpful comments and suggestions during peer-review. We also thank Yizhi Liu for their technical supports in the laboratory about the EPMA measurements. Discussion with Shen Shang is also appreciated.

References

Agee, C. B., Wilson, N. V., McCubbin, F. M., Ziegler, K., Polyak, V. J., Sharp, Z. D., et al. (2013). Unique meteorite from early Amazonian Mars: Water-rich basaltic breccia Northwest Africa 7034. *Science*, *339*(6121), 780–785. https://doi.org/10.1126/science.1228858

Al-Kathiri, A., Hofmann, B. A., Jull, A. T., & Gnos, E. (2005). Weathering of meteorites from Oman: Correlation of chemical and mineralogical weathering proxies with 14C terrestrial ages and the influence of soil chemistry. *Meteoritics & Planetary Science*, *40*(8), 1215–1239.

Arvidson, R. E., Squyres, S. W., Morris, R. V., Knoll, A. H., Gellert, R., Clark, B. C., et al. (2016). High concentrations of manganese and sulfur in deposits on Murray Ridge, Endeavour Crater, Mars. *American Mineralogist*, *101*(6), 1389–1405. https://doi.org/10.2138/am-2016-5599

Bernardini, S., Bellatreccia, F., Della Ventura, G., & Sodo, A. (2021). A reliable method for determining the oxidation state of manganese at the microscale in Mn oxides via Raman spectroscopy. *Geostandards and Geoanalytical Research*, *45*(1), 223–244. https://doi.org/10.1111/ggr.12361

Bhartia, R., Beegle, L. W., DeFlores, L., Abbey, W., Hollis, J. R., Uckert, K., & Zan, J. (2021). Perseverance's Scanning Habitable Environments with Raman and Luminescence for Organics and Chemicals (SHERLOC) investigation. *Space Science Reviews*, *217*(4), 1–115.

Bland, P. A., Zolensky, M. E., Benedix, G. K., & Sephton, M. A. (2006). Weathering of chondritic meteorites. *Meteorites and the Early Solar System II*, *1*, 853–868. https://doi.org/10.2307/j.ctv1v7zdmm.45

Crerar, D. A., Cormik, R. K., & Barnes, H. L. (1980). In I. M. Varentsov, & G. Gasselly (Eds.), *Geochemistry of manganese: An overview, geology and geochemistry of manganese* (Vol. 1, pp. 293–334). Stuttgart, Germany: E. Schweizerbart.

Crumpler, L. S., Arvidson, R. E., Mittlefehldt, D. W., Grant, J. A., & Farrand, W. H. (2020). Results from the first geologic traverse on the topographic rim of a complex impact crater, Endeavour Crater, Mars. *Geology*, *48*(3), 252–257. https://doi.org/10.1130/g46903.1

Ehlmann, B. L., & Edwards, C. S. (2014). Mineralogy of the Martian surface. *Annual Review of Earth and Planetary Sciences*, *42*, 291–315. https://doi.org/10.1146/annurev-earth-060313-055024

Gattacceca, J., Bouvier, A., Grossman, J., Metzler, K., & Uehara, M. (2019). The meteoritical bulletin, No. 106. *Meteoritics & Planetary Science*, *54*(2), 469–471. https://doi.org/10.1111/maps.13215

Hewins, R. H., Zanda, B., Humayun, M., Nemchin, A., Lorand, J. P., Pont, S., et al. (2017). Regolith breccia Northwest Africa 7533: Mineralogy and petrology with implications for early Mars. *Meteoritics & Planetary Science*, *52*(1), 89–124. https://doi.org/10.1111/maps.12740

Hurowitz, J. A., & McLennan, S. M. (2007). A~ 3.5 Ga record of water-limited, acidic weathering conditions on Mars. *Earth and Planetary Science Letters*, *260*(3–4), 432–443. https://doi.org/10.1016/j.epsl.2007.05.043

Hyde, B. C., Day, J. M., Tait, K. T., Ash, R. D., Holdsworth, D. W., & Moser, D. E. (2014). Characterization of weathering and heterogeneous mineral phase distribution in brachinite Northwest Africa 4872. *Meteoritics & Planetary Science*, *49*(7), 1141–1156. https://doi.org/10.1111/maps.12320

Koyama, S., Terada, N., Nakagawa, H., Kuroda, T., & Sekine, Y. (2021). Stability of atmospheric redox states of early Mars inferred from time response of the regulation of H and O losses. *The Astrophysical Journal*, *912*(2), 135. https://doi.org/10.3847/1538-4357/abf0ac

Lamm, S. N., Lanza, N. L., Gasda, P. J., Wiens, R. C., Meslin, P. Y., & Kirk, M. F. (2018). Manganese observations from ChemCam during Sols 1650-1750: Implications for a changing redox environment. In *Lunar and planetary science conference* (No. 2083, p. 2903).

Lanza, N. L., Fischer, W. W., Lamm, S. N., Gasda, P. J., Meslin, P. Y., Ollila, A. M., et al. (2019). Manganese on Mars as an indicator of habitable environments and as a biosignature. *LPI Contributions*, *2089*, 6445.

Lanza, N. L., Fischer, W. W., Wiens, R. C., Grotzinger, J., Ollila, A. M., Cousin, A., et al. (2014). High manganese concentrations in rocks at Gale crater, Mars. *Geophysical Research Letters*, *41*, 5755–5763. https://doi.org/10.1002/2014GL060329

Lanza, N. L., Gasda, P., Ari, E., Comellas, J., Caravaca, G., Rampe, E. B., et al. (2021). Chemistry of manganese-bearing materials at the Groken drill site, Gale Crater, Mars. In *52nd lunar and planetary science conference*.

Lanza, N. L., Wiens, R. C., Arvidson, R. E., Clark, B. C., Fischer, W. W., Gellert, R., et al. (2016). Oxidation of manganese in an ancient aquifer, Kimberley formation, Gale crater, Mars. *Geophysical Research Letters*, *43*(14), 7398–7407. https://doi.org/10.1002/2016gl069109

Lee, M. R., & Bland, P. A. (2004). Mechanisms of weathering of meteorites recovered from hot and cold deserts and the formation of phyllosilicates. *Geochimica et Cosmochimica Acta*, *68*(4), 893–916. https://doi.org/10.1016/s0016-7037(03)00486-1

Liu, Y., Fischer, W. W., Ma, C., Beckett, J. R., Tschauner, O., Guan, Y., et al. (2021). Manganese oxides in Martian meteorites Northwest Africa (NWA) 7034 and 7533. *Icarus*, *364*, 114471. https://doi.org/10.1016/j.icarus.2021.114471

Liu, Y., Ma, C., Fischer, W. W., Guan, Y., Webb, S. M., Beckett, J. R., et al. (2017). *Evidence of O_2-rich environments on Mars from hydrous Mn (IV)-oxides in Northwest Africa (NWA) 7034 and 7533 meteorites*.

Maynard, J. B. (2010). The chemistry of manganese ores through time: A signal of increasing diversity of earth-surface environments. *Economic Geology*, *105*(3), 535–552. https://doi.org/10.2113/gsecongeo.105.3.535

McCubbin, F. M., Boyce, J. W., Novák-Szabó, T., Santos, A. R., Tartèse, R., Muttik, N., et al. (2016). Geologic history of Martian regolith breccia Northwest Africa 7034: Evidence for hydrothermal activity and lithologic diversity in the Martian crust. *Journal of Geophysical Research: Planets*, *121*(10), 2120–2149. https://doi.org/10.1002/2016je005143

Meslin, P. Y., Gasda, P., L'Haridon, J., Forni, O., Lanza, N., Lamm, S., et al. (2018). Detection of hydrous manganese and iron oxides with variable phosphorus and magnesium contents in the lacustrine sediments of the Murray formation, Gale, Mars. In *Lunar and planetary science conference* (No. 2083, p. 1447).

Noda, N., Imamura, S., Sekine, Y., Kurisu, M., Fukushi, K., Terada, N., & Hartmann, J. (2019). Highly oxidizing aqueous environments on early Mars inferred from scavenging pattern of trace metals on manganese oxides. *Journal of Geophysical Research: Planets*, *124*(5), 1282–1295. https://doi.org/10.1029/2018je005892

Post, J. E. (1999). Manganese oxide minerals: Crystal structures and economic and environmental significance. *Proceedings of the National Academy of Sciences of the United States of America*, *96*(7), 3447–3454. https://doi.org/10.1073/pnas.96.7.3447

Roszjar, J., Metzler, K., Bischoff, A., BARRAT, J. A., Geisler, T., Greenwood, R. C., et al. (2011). Thermal history of Northwest Africa 5073––A coarse-grained Stannern-trend eucrite containing cm-sized pyroxenes and large zircon grains. *Meteoritics & Planetary Science*, *46*(11), 1754–1773. https://doi.org/10.1111/j.1945-5100.2011.01265.x

Santos, A. R., Agee, C. B., McCubbin, F. M., Shearer, C. K., Burger, P. V., Tartese, R., & Anand, M. (2015). Petrology of igneous clasts in Northwest Africa 7034: Implications for the petrologic diversity of the Martian crust. *Geochimica et Cosmochimica Acta*, *157*, 56–85. https://doi.org/10.1016/j.gca.2015.02.023

Saunier, G., Poitrasson, F., Moine, B., Gregoire, M., & Seddiki, A. (2010). Effect of hot desert weathering on the bulk-rock iron isotope composition of L6 and H5 ordinary chondrites. *Meteoritics & Planetary Science*, *45*(2), 195–209. https://doi.org/10.1111/j.1945-5100.2010.01017.x

Stephen, N. R. (2018). Linking martian breccias Northwest Africa 11220 and Northwest Africa 7034 to the martian meteorite family; Revisiting the martian nomenclature. In *Lunar and planetary science conference* (No. 2083, p. 1460).

Tebo, B. M., Johnson, H. A., McCarthy, J. K., & Templeton, A. S. (2005). Geomicrobiology of manganese(II) oxidation. *Trends in Microbiology*, *13*(9), 421–428. https://doi.org/10.1016/j.tim.2005.07.009

Thomas-Keprta, K. L., Clemett, S. J., Mckay, D. S., Gibson, E. K., & Wentworth, S. J. (2009). Origins of magnetite nanocrystals in martian meteorite ALH84001. *Geochimica et Cosmochimica Acta*, *73*(21), 6631–6677. https://doi.org/10.1016/j.gca.2009.05.064

Wittmann, A., Korotev, R. L., Jolliff, B. L., Irving, A. J., Moser, D. E., Barker, I., & Rumble, D., III. (2015). Petrography and composition of martian regolith breccia meteorite Northwest Africa 7475. *Meteoritics & Planetary Science*, *50*(2), 326–352. https://doi.org/10.1111/maps.12425

Wordsworth, R., Knoll, A. H., Hurowitz, J., Baum, M., Ehlmann, B. L., Head, J. W., & Steakley, K. (2021). A coupled model of episodic warming, oxidation and geochemical transitions on early Mars. *Nature Geoscience*, *14*(3), 127–132. https://doi.org/10.1038/s41561-021-00701-8

Wray, J. J. (2013). Gale crater: The Mars science laboratory/curiosity rover landing site. *International Journal of Astrobiology*, *12*(1), 25–38. https://doi.org/10.1017/s1473550412000328

Zeng, X., Li, S., Joy, K. H., Li, X., Liu, J., Li, Y., & Wang, S. (2020). Occurrence and implications of secondary olivine veinlets in lunar highland breccia Northwest Africa 11273. *Meteoritics & Planetary Science*, *55*(1), 36–55.

Zeng, X., Wu, Y., Zhao, Y. S., Pang, R., Mo, B., Wen, Y., et al. (2021). *Revealing high-manganese material on Mars at microscale [Dataset]. Figshare*. https://doi.org/10.6084/m9.figshare.15088566